Journal of Physics: Conference Series **1390** (2019) 012115 doi:10.1088/1742-6596/1390/1/012115

# Measurement of the energy spectra and of the angular distribution of the Transition Radiation with a silicon strip detector

**F Loparco[1,2], J Alozy[3], N Belyaev[4], M Campbell[3], M Cherry[5], F Dachs[3,6], S Doronin[4], K Filippov[4], P Fusco[1,2], F Gargano[2], E Heijne[3], S Konovalov[7], D Krasnopevtsev[4], X Llopart[3], V Mascagna[8,9], M N Mazziotta[2], H Pernegger[3], D Ponomarenko[4], M Prest[8,9], D Pyatiizbyantseva[4], R Radomskii[4], C Rembser[3], A Romaniouk[4], A A Savchenko[3,10], D Schaefer[11], E J Schioppa[3], D Shchukin[7], D Yu Sergeeva[4,10], E Shulga[4], S Smirnov[4], Y Smirnov[4], M Soldani[8,9], P Spinelli[1,2], M Strikhanov[4], P Teterin[4], V Tikhomirov[7], A A Tishchenko[4,10], E Vallazza[12], M van Beuzekom[13], B van der Heijden[13], K Vorobev[4] and K Zhukov[7]**

[1] Dipartimento di Fisica "M. Merlin" dell'Università e del Politecnico di Bari, Via G. Amendola 173, 70126 Bari, Italy
[2] Istituto Nazionale di Fisica Nucleare, Sezione di Bari, Via E. Orabona 4, 70126 Bari, Italy
[3] CERN, the European Organization for Nuclear Research, Esplanade des Particules 1, 1211 Geneva, Switzerland
[4] National Research Nuclear University MEPhI (Moscow Engineering Physics Institute), Kashirskoe highway 31, Moscow, 115409, Russia
[5] Dept. of Physics & Astronomy, Louisiana State University, Baton Rouge, LA 70803 USA
[6] Technical University of Vienna, Karlsplatz 13, 1040 Vienna, Austria
[7] P. N. Lebedev Physical Institute of the Russian Academy of Sciences, Leninsky prospect 53, Moscow, 119991, Russia
[8] INFN Milano Bicocca, Piazza della Scienza 3, 20126 Milano
[9] Universitá degli Studi dell'Insubria, Via Valleggio 11, 22100, Como
[10] National Research Center "Kurchatov Institute", Akademika Kurchatova pl. 1, Moscow, Russia
[11] University of Chicago, 5801 S Ellis Ave, Chicago IL 60637, USA
[12] INFN Trieste, Padriciano 99, 34149 Trieste, Italy
[13] Nikhef, Science Park 105, 1098 XG Amsterdam, The Netherlands

E-mail: `francesco.loparco@ba.infn.it`

**Abstract.** We plan to develop an advanced Transition Radiation Detector (TRD) for hadron identification in the TeV momentum range, based on the simultaneous measurement of the energies and of the emission angles of the Transition Radiation (TR) X-rays with respect to the radiating particles. To study the feasibility of this project, we have carried out a beam test campaign at the CERN SPS facility with 20 GeV/c electrons and muons up to 300 GeV/c. To detect the TR X-rays and the radiating particles, we used a 300 $\mu$m thick double-sided silicon strip detector, with a strip readout pitch of 50 $\mu$m. A 2 m long helium pipe was placed between the radiators and the detector, in order to ensure adequate separation between the TR X-rays and the radiating particle on the detector plane and to limit the X-ray absorption before the detector. We measured the double-differential (in energy and angle) spectra of the TR emitted

by several radiators. The results are in good agreement with the predictions obtained from the TR theory.

## 1. Introduction

Identification of high-energy hadrons is one of the most demanding challenges for the design of future detectors for both accelerator and cosmic-ray physics applications. An example is the planned Small Angle Spectrometer (SAS) experiment at the Large Hadron Collider (LHC), aimed to measure the inclusive cross sections in the forward region for the production of charged particles in proton-proton, proton-nucleus and nucleus-nucleus interactions at center-of-mass energies of 14 TeV [1]. In these collisions, secondary hadrons (mainly pions, kaons, protons) with momenta in the TeV range are produced, and the identification of the various species of particles can be definitely complex.

The only technique which allows hadron identification in the TeV region is based on the properties of the transition radiation (TR) [2]. TR can be emitted in the X-ray region whenever a ultrarelativistic charged particle crosses the boundary between two media with different dielectric constants. A typical Transition Radiation Detector (TRD) consists of a "radiator" followed by a X-ray detector. Since the average number of TR X-rays emitted at each interface is small, radiators consisting of multiple foils are employed to enhance the TR yield. The most common choice is that of using periodic radiators, consisting of multiple foils separated by air gaps (typical thickness of a few tens of $\mu$m for the foils and from a fraction to a few mm for the gaps). A periodic radiator introduces a threshold and a saturation value on the Lorentz factor (indicated with $\gamma_{th}$ and $\gamma_{sat}$) for the TR production, which depend on the foil and gap thicknesses; the interval $[\gamma_{th}, \gamma_{sat}]$ can even span over a decade. This feature allows discrimination of fast radiating particles from slower nonradiating ones [3]. Irregular radiators (fibers or foams) are also widely used, since they exhibit a behavior fairly similar to that of regular ones, and in addition they allow isotropic and self-supporting structures.

TRDs are widely used for electron-hadron separation in high-energy physics experiments [4–6] and work efficiently for momenta up to about 1 TeV/c. Hadron identification with TRDs is more complex, since the relative differences between the hadron masses are smaller. Nonetheless, in the past several TRD prototypes were developed to identify pions, kaons and protons with momenta up to 200 GeV/c [7–11]. In a conventional TRD, the different species of particles are identified either using the information about the energy deposited in the detector, which includes the energies of the absorbed TR X-rays and the ionization energy loss ($dE/dx$) of the particle, or by counting the candidate TR photons.

A possible option to enhance the performance of a TRD is that of measuring simultaneously the number of TR X-rays, their energies and their emission angles with respect to the radiating particles. To implement this option, particular care should be taken in the choice of the detector and of the radiator as well as in the optimization of the geometry. As starting point, a high-efficiency and high-granularity X-ray detector is required, and its efficiency curve should match with the production spectrum of TR X-rays in the radiator. In addition, since TR photons are emitted at small angles with respect to the radiating particle ($\theta \sim 1/\gamma$), the distance of the detector from the radiator should be chosen in order to ensure adequate separation between the TR photons and the particle on the detector plane.

To test the possibility of implementing this option, we have performed a test beam at the CERN SPS facility using a double-face silicon strip detector (DSSD). In this paper the preliminary results of the test beam will be reported. Similar measurements were also performed using a silicon pixel detector [12].

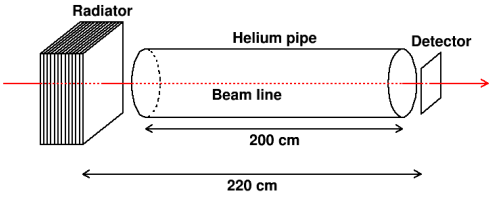


**Figure 1.** Schematic view of the test beam setup.

## 2. Test beam at the CERN SPS

For our test beam we used a double-side high-resistivity 300 $\mu$m thick silicon micro-strip detector with a sensitive area of $1.92 \times 1.92\,\mathrm{cm}^2$ [13]. The detector $p$-side ("junction side") is equipped with 768 $\mathrm{p}^+$ strips, with a pitch of 25 $\mu$m and with a readout pitch of 50 $\mu$m. A readout scheme with one floating strip is therefore implemented. The $n$-side ("ohmic side") is equipped with 384 $\mathrm{n}^+$ strips, orthogonal to those on the junction side, with a pitch of 50 $\mu$m. All the strips on the ohmic side are readout. Hence the detector has 384 readout strips with a 50 $\mu$m pitch on both sides.

We performed our measurements at the CERN-SPS H8 facility, using a 20 GeV/c mixed electron-pion beam and muon beams with momenta of 290 GeV/c, 180 GeV/c and 120 GeV/c. Figure 1 shows a schematic view of the experimental setup. The silicon detector was located 220 cm downstream the radiator, with the junction side facing to the radiator. A 200 cm long helium pipe was placed after the radiator to minimize X-ray absorption along the path to the detector. A trigger system consisting of a set of scintillator counters, an upstream Cherenkov counter, a preshower detector and a lead glass calorimeter was implemented to separate particles of different types. A multiplicity counter was used as veto to remove upstream showers and multi-particle events.

We have tested several periodic and irregular radiators. In the following sections we will discuss the results obtained with a radiator consisting of 30 mylar foils, 50 $\mu$m thick separated by 2.97 mm air gaps. In order to measure the background due to non-TR X-rays or delta-rays produced by the beam particles interacting upstream the detector, we also took some data without radiators or with a "dummy" radiator, e.g. a polyethylene slab with the same thickness (in radiation length units) as the mylar radiator.

Dedicated pedestal runs have been also performed to evaluate the detector noise. The average noise level, evaluated from the rms of the pedestal distributions, is of about 1.39 keV for the strips on the junction side and of about 1.78 keV for those on the ohmic side[1]. Noisy strips are also identified in pedestal runs and are masked in the data analysis.

## 3. Data analysis

A charged particle crossing the detector will induce electrical signals on a cluster of adjacent strips. We define a particle cluster starting from a "seed", i.e. a strip with a Signal-to-Noise level $S/N > 20$, and associating to it all the adjacent strips with $S/N > 3$. An additional cut $S/N > 30$ for the total charge of the cluster is required. For our analysis we select a sample

[1] The noise level is expressed in energy units using the results of the calibration procedure described in Section 3.

of events with only one particle cluster on both sides of the detector. This selection makes it possible to unambiguously match the particle clusters on the two sides; the particle is therefore assigned the coordinates of the centers of gravity of the two clusters.

Energy calibration is performed by fitting the ADC count distributions of particle clusters with a Landau distribution and assuming that the most probable ionization energy loss of 290 GeV/c muons in 300 $\mu$m silicon is 83.5 keV (see Ref. [14])[2].

X-ray clusters are defined in a way similar to particle clusters. In this case we start from a seed strip with $S/N > 4$ and we associate to it all adjacent strips with $S/N > 1$. Due to this choice, the average energy thresholds for X-ray clusters are of 5.6 keV on the junction side and of 7.1 keV on the ohmic side. For each X-ray cluster on the two detector sides, a separation of at least one strip from the particle cluster and from other X-ray clusters is also required.

In our analysis we select events with only one X-ray cluster on both detector sides. As for the particle clusters, this selection allows unambiguous matching of the X-ray clusters on the two sides; each candidate X-ray is therefore assigned the coordinates of the centers of gravity of the two X-ray clusters. Finally, the values of the particle energy and of the X-ray energy are taken from the clusters on the junction side, which exhibits a lower noise level than the ohmic side.

## 4. Results and discussion

Figure 2 shows a summary of the results obtained with 20 GeV/c electrons. From our data we have evaluated the double-differential spectrum $d^2N/d\theta d\omega$ of the TR X-rays emitted by the mylar radiator as a function of the photon energy $\omega$ and of the emission angle $\theta$. The spectra shown in the figure have been obtained applying the analysis procedure described in Sec. 3 and subtracting the background, evaluated in a dedicated run with the dummy radiator.

To provide an interpretation of the data, we have developed a custom Monte Carlo code which includes a full simulation of the physics processes and of the detector response. The double-differential spectrum $d^2N/d\theta d\omega$ of the TR X-rays absorbed in the detector is calculated after folding the production spectrum, which is evaluated from the conventional formulas in Ref. [15], with the absorption of X-rays along their path from the radiator to the detector. The values of the absorption lengths of the various materials have been taken from the NIST reference database [16].

The energy deposition of each particle in the detector is extracted from a Landau distribution with a most probable value of 83.5 keV. The number of hit strips on two detector sides are extracted from the strip multiplicity distributions of particle clusters in real data. The energy deposited by the particle is then shared among these strips according to a Gaussian profile, with larger fractions of energy associated to the strips closer to the impact point. The number of TR X-rays associated to each particle is then extracted from a Poisson distribution with an average value corresponding to the integral of the simulated TR spectrum absorbed in the detector. The energy $\omega$ and the polar angle $\theta$ of each photon with respect to the direction of the radiating particle are randomly extracted from the double-differential spectrum $d^2N/d\theta d\omega$, while the azimuth angle $\phi$ is extracted from a uniform distribution in $[0, 2\pi]$. The generation point of each TR photon is randomly chosen along the particle track within the radiator, and the photon is then propagated to the detector. The photon energy is then shared between the two strips on each detector side which are closest to the X-ray absorption point. This corresponds to the hit multiplicity observed in data. The detector noise is finally taken into account in the simulations, adding to each strip a noise charge according to the measured values in the pedestal runs. The simulated data are then analyzed applying the same algorithm as in real data.

[2] The most probable value of the energy loss is not significantly different for 20 GeV/c electrons and for 180 GeV/c and 120 GeV/c muons.

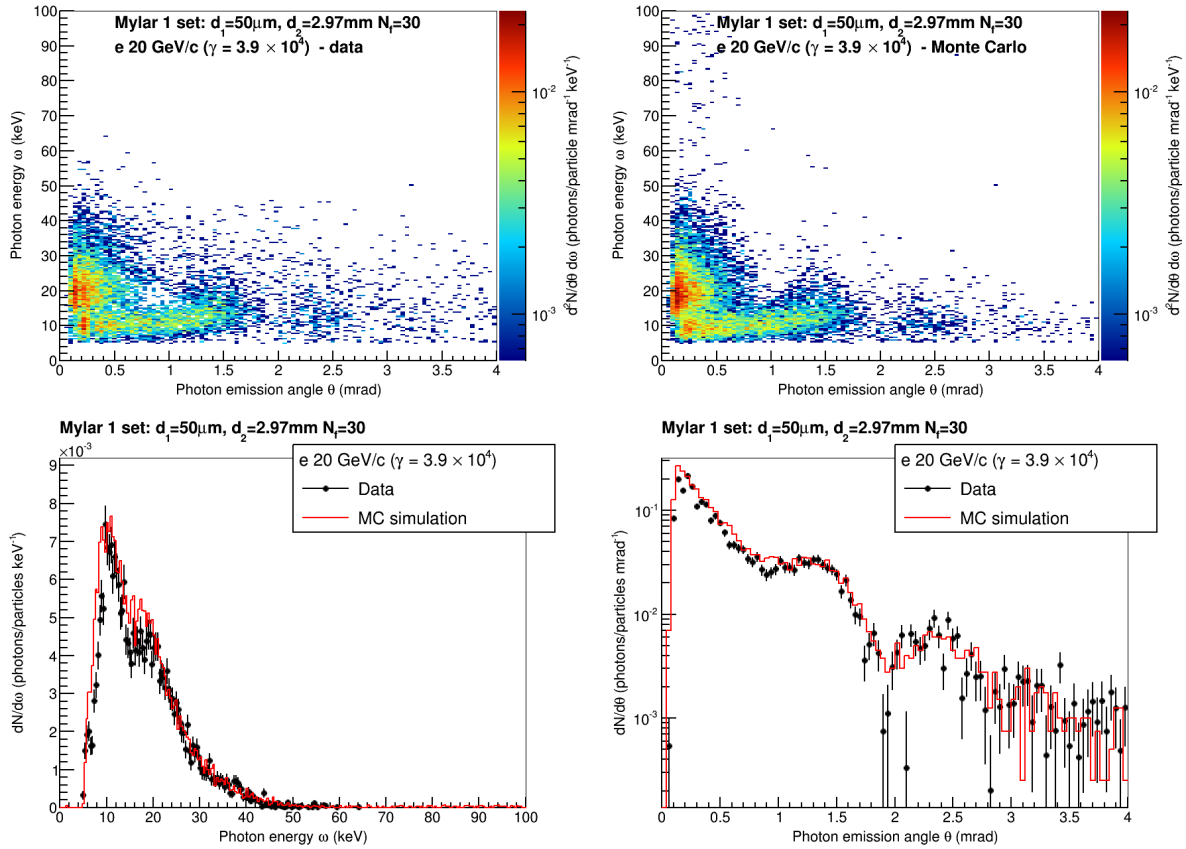


**Figure 2.** Results of the measurements with 20 GeV/c electrons and comparison with the predictions from the Monte Carlo simulation. Top panels: measured (left) and simulated (right) double-differential spectra (in energy and angle) of the TR X-rays. Bottom left panel: TR X-ray differential energy spectrum. Bottom right panel: TR X-ray differential angular spectrum.

A comparison between the measured and the simulated double-differential spectrum of the TR X-rays is shown in the top panels of Fig. 2. The data confirm that the highest energy photons ($\omega > 15$ keV) are mostly emitted at small angles with respect to the radiating particle, while the lower energy ones are spread over angles significantly larger than $1/\gamma$. In the bottom panels of Fig. 2 we show the comparison between the measured and the simulated energy and angular differential spectra of the TR X-rays. The simulation reproduces the experimental data fairly well, although some small discrepancies are observed. In particular, the simulation predicts a slight excess of photons with energies above 15 keV with respect to the data. This is also seen in the angular spectrum, where the structure with multiple peaks is correctly reproduced by the simulation, but the first peak below 0.3 mrad is more populated than in data. These discrepancies can originate from an inaccurate representation of the material thicknesses and of the X-ray absorption lengths implemented in the simulation. The same considerations apply to the results obtained in the muon runs, which are summarized in Fig. 3.

## 5. Conclusions

We have mesaured the energy and emission angles of TR X-rays produced by fast particles crossing a mylar radiator using a double-sided silicon strip detector. The test has been performed

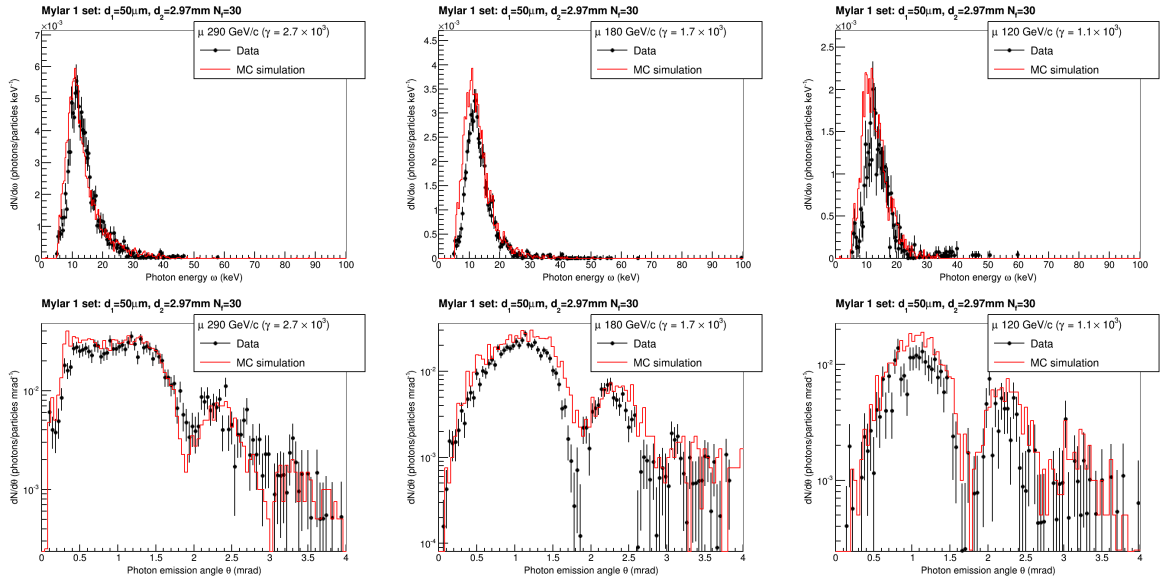


**Figure 3.** Results of the measurements with 290, 180 and 120 GeV/c muons and comparison with the predictions from the Monte Carlo simulation. Top panels: TR X-ray differential energy spectra. Bottom panels: TR X-ray differential angular spectra.

with a beam of particles covering a range of Lorentz factors from about $10^3$ to about $4\times10^4$. The test beam data have been compared with the predictions of a custom Monte Carlo simulation based on the parameterizations of the TR yield derived from theoretical calculations. The measured energy and angular distributions of TR X-rays are well reproduced by the simulation.

## Acknowledgments

We gratefully acknowledge the financial support from Russian Science Foundation grant (project No. 16-12-10277).

## References

[1] Albrow M 2018 (*Preprint* `1811.02047`)
[2] Ginzburg V L and Frank I M 1945 *J. Phys.(USSR)* **9** 353–362 [1946 *Zh. Eksp. Teor. Fiz.* **16** 15]
[3] Patrignani C *et al.* (Particle Data Group) 2016 *Chin. Phys. C* **40** 100001
[4] Aad G *et al.* (ATLAS) 2008 *JINST* **3** S08003
[5] Aamodt K *et al.* (ALICE) 2008 *JINST* **3** S08002
[6] Kirn T (AMS 02 TRD) 2013 *Nucl. Instrum. Meth. A* **706** 43–47
[7] Fabjan C W *et al.* 1981 *Nucl. Instrum. Meth.* **185** 119
[8] Oganesian A G, Sarkisian A S and Atac M 1977 *Nucl. Instrum. Meth.* **145** 251
[9] Commichau V, Deutschmann M, Goddeke H, Hangarter K, Putzhofen U, Schulte R and Struczinski W 1980 *Nucl. Instrum. Meth.* **176** 325–331
[10] Deutschmann M *et al.* 1981 *Nucl. Instrum. Meth.* **180** 409
[11] Ludlam T *et al.* 1981 *Nucl. Instrum. Meth.* **180** 413
[12] Schioppa E J *et al.* 2018 *Accepted by Nucl. Instrum. Meth. A* Doi: `10.1016/j.nima.2018.11.062`
[13] Lietti D, Berra A, Prest M and Vallazza E 2013 *Nucl. Instrum. Meth. A* **729** 527–536
[14] Bichsel H 1988 *Rev. Mod. Phys.* **60** 663–699
[15] Cherry M L, Hartmann G, Muller D and Prince T A 1974 *Phys. Rev. D* **10** 3594–3607
[16] `https://www.nist.gov/pml/x-ray-mass-attenuation-coefficients`